European Polymer Journal 99 (2018) 445–455
https://doi.org/10.1016/j.eurpolymj.2017.12.045

PLA/PCL ELECTROSPUN MEMBRANES OF TAILORED FIBRES DIAMETER AS DRUG DELIVERY SYSTEMS

M. Herrero Herrero[1], J.A. Gómez-Tejedor[1,2], A. Vallés-Lluch[1,*]

[1] Centre for Biomaterials and Tissue Engineering, Universitat Politècnica de València, Cno. de Vera s/n, 46022, Valencia, Spain

[2] Biomedical Research Networking Center in Bioengineering, Biomaterials and Nanomedicine (CIBER-BBN), Valencia, Spain

** Corresponding author. E-mail address: avalles@ter.upv.es*

European Polymer Journal 99 (2018) 445–455

https://doi.org/10.1016/j.eurpolymj.2017.12.045

European Polymer Journal 99 (2018) 445–455
https://doi.org/10.1016/j.eurpolymj.2017.12.045

Abstract

The main electrospinning parameters, *i.e.*, polymer concentration in the injectable solution, solvents used and their proportion, flow rate, voltage and distance to collector were herein systematically modified to analyse their particular influence in fibres diameter of electrospun membranes of poly(lactic acid), polycaprolactone and their mixture. As a result of this analysis, the procedures to obtain membranes of these polymers and blend with under- and above-micron-sized fibres were established, in which the solvents ratio (chloroform/methanol and dichloromethane/dimethylformamide) and voltage were found to play the major role. Moreover, the plausible differential effect of these fibres diameters (0.8 and 1.8 μm) in the controlled release of a molecule of interest was explored, using bovine serum albumin (BSA), proving that the most effective configuration for BSA release among those studied was the PLA-PCL combination in membranes of above-micron fibres diameter.

Keywords: polylactic acid, polycaprolactone, electrospinning, drug delivery, membrane

European Polymer Journal 99 (2018) 445–455
https://doi.org/10.1016/j.eurpolymj.2017.12.045

1. INTRODUCTION

Polylactic acid (PLA) is a highly versatile, aliphatic polyester, [1] biocompatible and biodegradable at a slow rate. It is present in three isomeric forms (D), (L), and racemic (D, L). P(L)LA and P(D)LA are semi-crystalline solids, easy to process and have been approved for biomedical applications by the U.S. Food and Drug Administration (FDA). [2] These properties have made PLA-based materials worthy for biomedical applications, including sutures, bone fixation implants, stents, scaffolds for tissue engineering and carriers for drug delivery. [1,3,4,5] For most applications, the (L) isomer (hereafter named PLLA) is chosen because it is preferentially metabolised in the body. [6]

Besides, polycaprolactone (PCL) is a synthetic biodegradable and bioresorbable polymer belonging also to the aliphatic polyesters family. [7] It is a hydrophobic, semi-crystalline polymer and its crystallinity tends to decrease as its molecular weight increases. [8] Because of its high crystallinity and high hydrophobicity, it degrades at a much slower rate than PLA. [6] PCL has also been approved by the FDA for clinical applications, and is extensively used in lots of biomedical applications due to the proper tensile property and biocompatibility, [9,10,11,12] pure or in combination with other polyesters in order to modulate its degradation kinetics.

In particular, scaffolds based on PLA or PCL and copolymers or blends thereof have been proposed in a wide variety of tissue engineering strategies because these polymers show ductile properties, can be easily processed to achieve different microarchitectures, and are safely reabsorbed. [13] Porous structures are obtained, for example by 3D printing, electrospinning, [14] selective laser sintering or fused deposition modelling. [15]

Among the techniques to fabricate scaffolds for tissue engineering applications, electrospinning stands out because the diameters of electrospun fibres can be of a similar magnitude to fibrils in the extracellular matrix (ECM) and consequently mimic

quite faithfully the natural cells environment. Thus, these scaffolds have shown to positively promote cell-matrix and cell-cell interactions with the cells having a normal phenotypic shape and gene expression. [16,17] As an example, Shakhssalim *et al.* explored the application of electrospun PLA/PCL scaffolds for bladder regeneration by culturing smooth muscle and urothelial cells. [18]

Moreover, electrospinning as a means of generating porous structures has many advantages:

1. It is a relatively robust and simple technique to produce nanofibres from a wide variety of polymers. [19]
2. Electrospun nanofibres present an extremely high surface-to-volume ratio and tuneable porosity, can be conformed to a wide variety of sizes and shapes and their composition can be tailored to achieve the desired properties and functionality. [20]
3. Nanofibres with high surface area and porosity have enormous scope for applications in engineering mechanically stable and biologically functional tissue scaffolds. The high surface-to-volume of the nanofibre provides more room for the cell attachment than the regular fibres. [21,16]
4. The parameters of electrospinning, such as polymer concentration, solvent, solvent ratio, flow rate, distance to collector and voltage have significant effect on the fibres morphology obtained, so by proper manipulation of these parameters nanofibres of desired morphology and diameters can be obtained. [22]

Although there are many works dealing with electrospinning of PLA/PCL blends, [23,24,25,26] up to now there are no thorough studies addressing the influence of the main electrospinning parameters (polymer concentration, solvent, solvent ratio, flow rate, voltage and collector distance) on fibre diameter. Thus, herein the aims were *i)* to assess

the influence of the parameters involved in the microarchitecture of electrospun membranes of PCL, PLA and PCL/PLA blends, namely the polymer concentration in the solvent mixture, solvents ratio in the mixture to electrospin, the flow rate, voltage and collector distance, and *ii)* to explore whether the fibres diameter may yield drug release variations. To this end, electrospun membranes of the three compositions were obtained, having two fixed average fibres diameter. These membranes were then manufactured with bovine serum albumin (BSA) added to the polymer mixture in order to follow its release over time and relate it with the morphology and chemical nature of the fibres.

2. MATERIALS AND METHODS

2.1. Preparation of solutions

The polymer solutions were obtained by stirring the polymers in appropriate solvents during 24 h. PLA (NatureWorks, INGEO 4042 D, pellet shape, Mw 2.8 x 10^5 Da), PCL (Sigma-Aldrich, pellet shape, Mw 70000-90000 g/mol), and a 50% w/w PLA/PCL mixture were mixed separately with chloroform (Scharlab, extrapure, stabilized with ethanol) and methanol (Scharlab, multisolvent) in the case of homopolymers, and dichloromethane (DCM; Scharlab, synthesis grade, stabilized with approximately 50 ppm of amylene) and dimethylformamide (DMF; Scharlab, synthesis grade) in the case of their blend, at different solvents ratios (66-33 to 80-20 %v/v) and polymer/solvent mixture ratios (5 to 23 %wt/v).

2.2. Manufacture of electrospun membranes

The polymer mixtures were electrospun using a home-made equipment for 30 min, to obtain membranes thick enough to be detached from the metal holder and be manipulated (around 300 μm). The equipment consists of a pump (RS-232, model NE 1000. New Era Pump Systems, Inc.) to which the syringe with the polymer solution was connected, a voltage source (OL400W-503. HiTek Power) and a metal collector covered by aluminium foil to improve the deposition of fibres. The voltage source is connected to the collector and the needle creating a differential of potential, which provokes the ejection of the polymer solution towards the collector. [27,28,29,30]

The main electrospinning parameters, concerning the polymer solution (polymer concentration in the solvents mixture, chloroform-methanol or DCM-DMF binary mixture, and solvents ratio in it) and the electrospinning process itself (flow rate, distance to collector and voltage applied) were systematically changed to avoid defects in the membranes, study their influence on the membranes' morphology, and tailor the fibre diameters to yield membranes of similar morphology but different chemistry, and two different enough fibre morphologies to likely lead to different drug release profiles. The membranes, electrospun on flat collectors covered with aluminium foil, were stored refrigerated in zip bags until use, and then demolded.

2.3. Preparation of films

Films were prepared by solvent-casting. Depending on the polymer concentration in the polymer solution, different volumes (4 to 10 ml) of these were poured in Petri dishes having 8 cm in diameter to obtain films with 100 μm thickness. The Petri dishes were covered with mesh fabrics to allow the solvent evaporation overnight. The films were demolded, with the help of water, and stored in the fridge until use.

2.4. Determination of the viscosity of the polymer solutions

The polymer solutions are non-newtonian fluids because their relation between shear stress and their strain rate is non-lineal. For that reason, they were characterised by their corresponding rheograms, which represent the rheological behaviour of the solutions. A parallel plate's rheometer (Discovery HR-2 hybrid rheometer, TA Instruments) was used for this purpose. 550 μl of polymer solution was measured each time, 3 replicates per composition. The rheograms were obtained at 25ºC by applying a shear ramp from 1 to 1500 s^{-1} during 1 min.

2.5. Determination of the solution's surface tension

Due to the high viscosity of the polymeric solutions and the volatility of their solvents, their surface tension could not be determined by the pendant drop method and contour analysis, and a technique based on Tate's law was followed instead.

Briefly, Tate's law is based on the balance between the weight of a pendant drop and the opposite force exerted by its surface tension. The weight makes the drop fall along the capillary but the surface tension provokes a force equilibrium that keeps the drop suspended from the tip of the capillary. [31]

As surface tension is proportional to the wet perimeter of the capillary border (it being the inner or outer perimeter, depending on the mixture) the following equation represents the equilibrium explained above:

$$m \cdot g = \gamma \cdot 2 \cdot \pi \cdot r$$

where m is the mass of the falling drop, g is the gravitational acceleration, γ is the surface tension at the drop-air interface, and $2\pi r$ is the wet perimeter. According to the characteristics of the liquid, r is the outer or inner radius of the capillary, depending on whether the drop pends or not, respectively.

Jordi Riba-Roger and Bernat Esteban added a correction factor *F* previously introduced by Earnshaw *et al.*, which relates the volume of the real drop with that of the ideal one by considering the dimensionless radius of the capillary: [31,32]

$$m \cdot g = F \cdot \gamma \cdot 2 \cdot \pi \cdot r$$

The mathematical approach for factor *F* was developed by Lee-Chan-Pogaku [33] as:

$$F = 1 - 0.9121 \cdot \left(\frac{r}{V^{\frac{1}{3}}}\right) - 2.109 \cdot \left(\frac{r}{V^{\frac{1}{3}}}\right)^2 + 13.38 \cdot \left(\frac{r}{V^{\frac{1}{3}}}\right)^3 - 27.29 \cdot \left(\frac{r}{V^{\frac{1}{3}}}\right)^4$$
$$+27.53 \cdot \left(\frac{r}{V^{\frac{1}{3}}}\right)^5 - 13.58 \cdot \left(\frac{r}{V^{\frac{1}{3}}}\right)^6 + 2.593 \cdot \left(\frac{r}{V^{\frac{1}{3}}}\right)^7$$

where *r* is the radius of the capillary and *V* is the volume of the drops weighed. This volume was obtained from their weight and the previously measured density, making use of a picnometer.

Taking this law into account, the assay was carried out with a Petri dish inside a balance chamber (Mettler Toledo AX205). The Petri dish was covered with parafilm to reduce the solvent evaporation and perforated to allow the pass of a glass micropipette. Five drops were slowly left on the Petri dish by using a micropipette and weighed. A calliper was used to measure the outer diameter of the micropipette used (1.6 mm) since the wetted surface includes the entire tip of the capillary.

2.6. BSA loading and release

The release of bovine serum albumin (BSA; cold ethanol fraction, pH 5.2, ≥96%, Sigma-Aldrich) was followed in aqueous medium using phosphate-buffered saline (PBS, Sigma Aldrich). For that purpose, analogous series of membranes and films loaded with BSA were prepared as previously described from polymer solutions to which BSA diluted in PBS was added. So, firstly a 500 mg/mL BSA solution in PBS

was prepared and left in the fridge to facilitate the dilution, avoiding the denaturation of the protein that stirring would cause. In parallel, the pair of solvents (DCM-DMF or chloroform-methanol) were mixed using Span80 surfactant (Sigma-Aldrich), at a final concentration of 40% wt with respect to BSA, because some of the solvents to electrospin are non-polar. The BSA/PBS solution was added dropwise to the solvents/surfactant mixture to finally obtain polymer solutions containing 12% wt of BSA with respect to the polymer, stirred for 30 min at 240 rpm, followed by the incorporation of the polymer and stirring overnight prior to electrospinning.

Once the membranes were obtained and detached from the aluminium foil and films were demolded from the Petri dishes, 20 mg of each were introduced in vials containing 2 ml of PBS. At pre-selected time intervals (up to 21 days), 0.5 ml of supernatant were withdrawn, replaced by 0.5 ml of new PBS, and stored in the freezer until its analysis. In parallel, the assay was followed with membranes and films non-loaded with BSA (henceforth blank).

Ultraviolet radiation spectroscopy was used for the BSA quantification analysis, which involves the previous reaction of the supernatant with the BCA reactant according to the manufacturer's (Micro BCA™ Protein Assay Kit. ThermoFisher Scientific) instructions. The protocol followed consisted in pouring 10 µL of each supernatant in a microtube, to which 200 µL of BCA reactant was added. To improve the reaction the microtubes were incubated at 37ºC for 1 h after their stirring during 30 s. Next, the microtubes were cooled at room temperature and stirred again for 30 s. Finally, samples were poured in a 96 multiwell plate to measure the absorbance at 570 nm in a VICTOR 1420 ultraviolet radiation spectrophotometer (PerkinElmer). This absorbance is proportional to the BSA concentration, being necessary to obtain previously a standard

calibration curve using different BSA solutions with known concentrations in PBS (0 to 1000 μg/mL).

The real absorbance of samples was obtained by subtracting the absorbance of blanks to those of loaded materials. Next, using the standard calibration curve, and making use of the supernatant volume and the volume withdrawn each time, the mass of BSA released at each time could be obtained and related to the initial mass in the materials, considering that the electrospun solution is homogeneous.

2.7. Morphology of the membranes

The morphology and the presence of defects in the nanostructure of the electrospun membranes were assessed in a JSM-5410 scanning electron microscope (SEM; JEOL. Ltd., Tokyo, Japan), at 15 kW of acceleration voltage and 9 mm of working distance. The samples were sputter-coated with gold under vacuum before observation.

Analysing the images with the help of the ImageJ software (National Institute of Health, Bethesda, Maryland, USA) it was possible to determine the mean diameter of the fibres; 30 different fibres were measured and measurements were repeated 3 times per fibre, at different points. The membranes with fibres diameter below 1 μm are hereafter named as U (under-micron fibres) and those with fibres above 1 μm in diameter are named as A (above-micron fibres).

2.4. Differential Scanning Calorimetry (DSC)

Thermal properties of the electrospun membranes and films were characterised using a Perkin Elmer DSC800 device. Approximately 4 mg of sample were sealed in aluminium pans with hole to permit the release of any gas formed, and their thermal behaviour was analysed in a temperature range from -60ºC to 200ºC at a heating rate of 20ºC/min.

The crystallinity of PCL and PLA in the samples, X_{PCL} and X_{PLA}, was calculated from the following equations [34]:

$$X_{PCL}(\%) = \frac{\Delta H_m}{\Delta H^{\infty}_{mPCL} \cdot W_{PCL}} \cdot 100$$

$$X_{PLA}(\%) = \frac{\Delta H_m - \Delta H_c}{\Delta H^{\infty}_{mPLA} \cdot W_{PLA}} \cdot 100$$

where W_{PCL} and W_{PLA} are the weight fractions of PCL and PLA (0.5 in the blend, and 1 for the pure materials), ΔH_m is the melting enthalpy of PCL or PLA, ΔH_c is the cold crystallization enthalpy of PLA, and ΔH^{∞}_{mPCL} and ΔH^{∞}_{mPLA} are the melting enthalpies of a 100% crystalline material, taken to be 93 J/g for PLA [35] and 139.5 J/g for PCL[36].

3. RESULTS AND DISCUSSION

3.1. Analysis of the influence of the main electrospinning parameters and selection of the ones leading to U and A membranes of similar fibres diameter

To firstly analyse the influence of the different parameters on the fibres morphology, a set of electrospun membranes were obtained in which all parameters were kept constant, except the one under study, which was changed monotonously. The manufactured membranes were observed under SEM and the mean diameter and standard deviation were calculated as stated before.

For the three polymers used, the influence of the main electrospinning parameters on the morphology of membranes thereof is represented in Figures 1, 2 and 3, and their effect on the fibres diameter is shown in Figure 4.

European Polymer Journal 99 (2018) 445–455
https://doi.org/10.1016/j.eurpolymj.2017.12.045

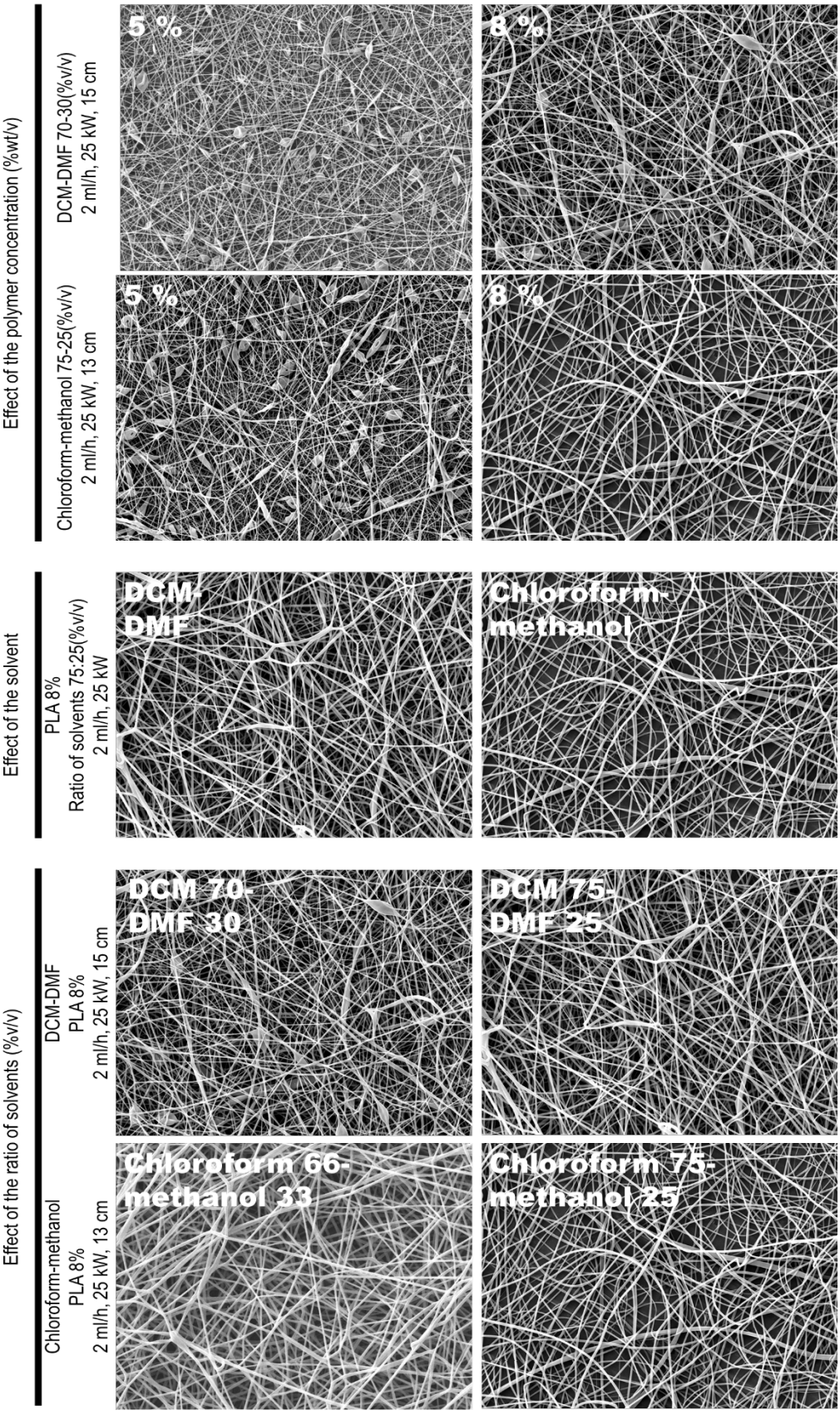

Figure 1. Effect of the main solution parameters on the morphology of electrospun PLA membranes: polymer concentration (%wt/v), solvents and ratio of solvents (%v/v).

European Polymer Journal 99 (2018) 445–455
https://doi.org/10.1016/j.eurpolymj.2017.12.045

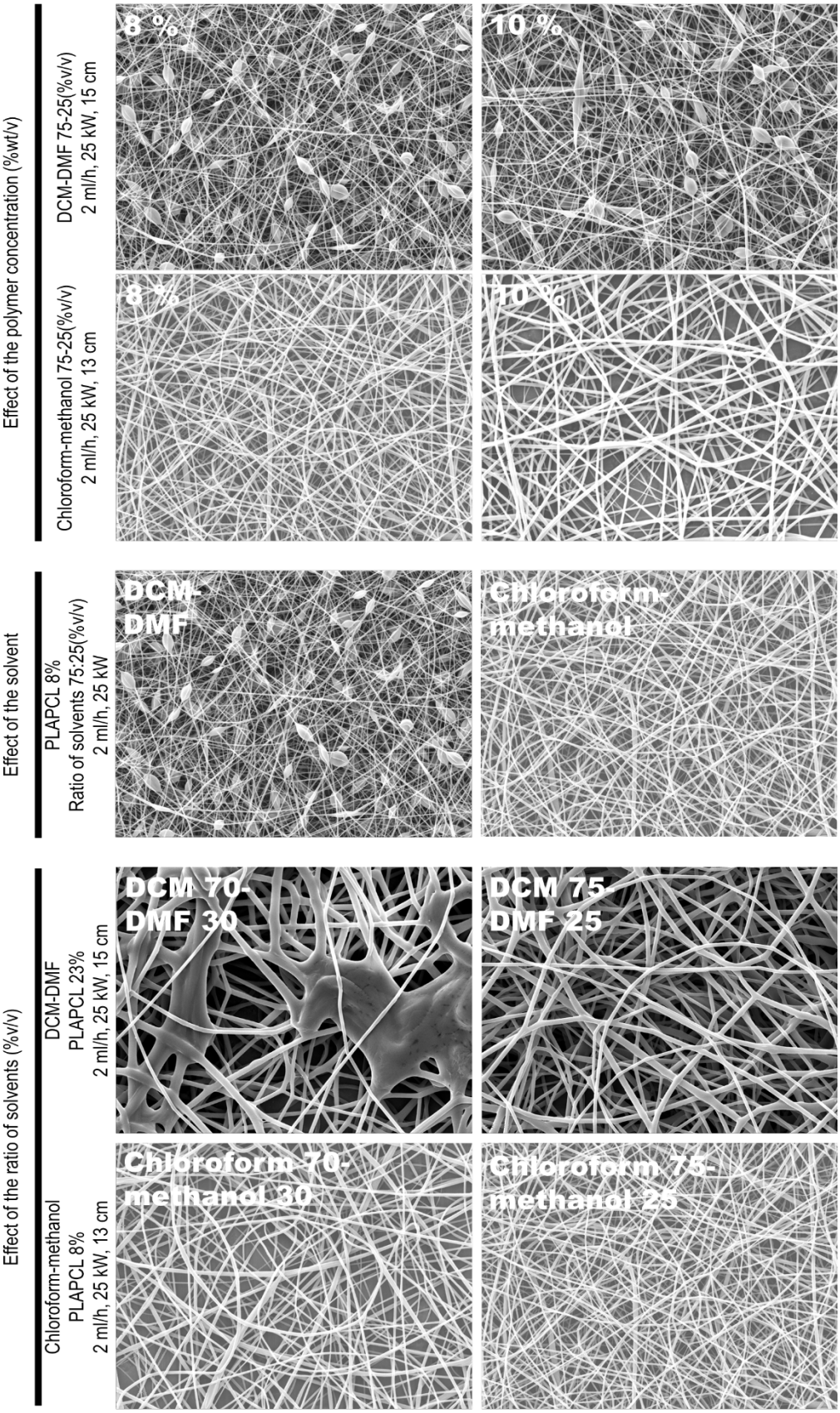

Figure 2. Effect of the main solution parameters on the morphology of electrospun PLA-PCL membranes: polymer concentration (%wt/v), solvents and ratio of solvents (%v/v).

European Polymer Journal 99 (2018) 445–455
https://doi.org/10.1016/j.eurpolymj.2017.12.045

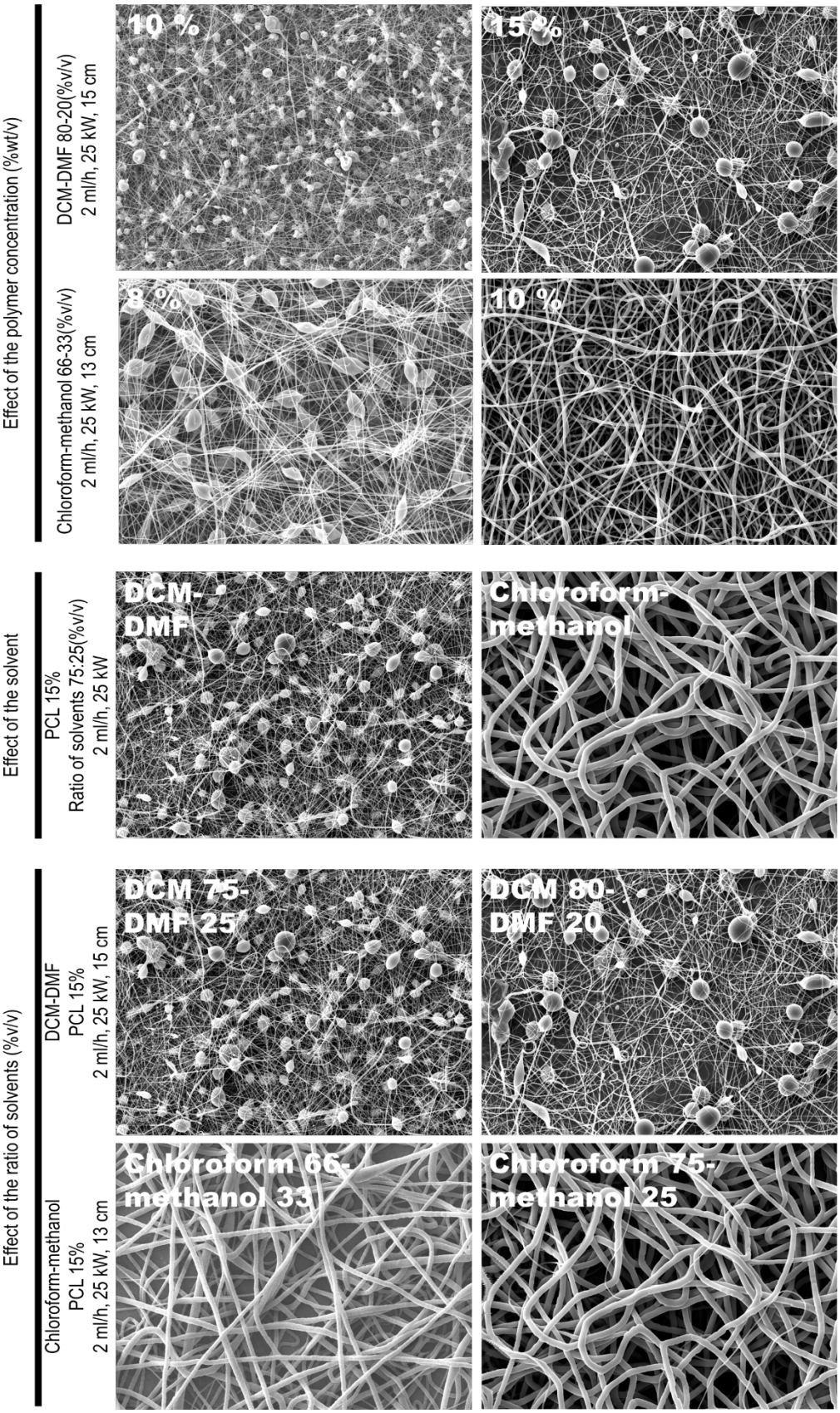

Figure 3. Effect of the main solution parameters on the morphology of electrospun PCL membranes: polymer concentration (%wt/v), solvents and ratio of solvents (%v/v).

European Polymer Journal 99 (2018) 445–455
https://doi.org/10.1016/j.eurpolymj.2017.12.045

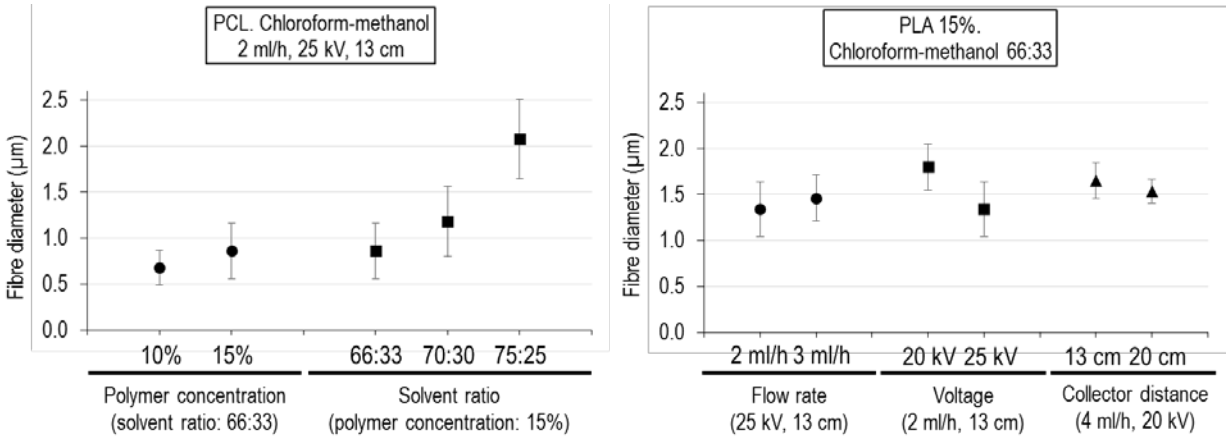

Figure 4. Effect of the main electrospinning parameters on fibres diameter: polymer concentration in the solvents mixture (%wt/v), chloroform-methanol solvents ratio (%v/v), flow rate (ml/h), voltage (kW) and distance to collector (cm).

Figures 1, 2 and 3 show that the solvent plays an important role in order to determine the rest of electrospinning parameters, mainly the polymer concentration. The DCM-DMF mixture demands a higher polymer concentration than chloroform-methanol. Moreover, the range of polymer concentrations varies depending on the polymer, being it higher for PCL because this polymer is less polar than PLA. The viscosity of the solution is related with the polarity of polymer, and the higher the viscosity the lower the number of defects in the electrospun membrane. Thus, PCL has a lower viscosity due to its lower polarity resulting in a better solubility in the solvents used when the non-polar solvent (be it DCM or chloroform) is predominant.

For a polymer concentration of 8%wt/v it is possible to obtain electrospun membranes without defects using PLA and PLA/PCL in chloroform-methanol, but when using PCL a greater concentration, of 10% wt/v, is needed. In DCM-DMF, PCL and PLA/PCL concentrations are to be higher than 15% wt/v and 10% wt/v, respectively.

For all polymers, the fibres diameter slightly increases with the increase of the polymer concentration in the solvent mixture. This is in agreement with the observations by Huang *et al.* [37] According to these authors, since nanofibres result from evaporation of polymer fluid jets, the fibres diameters depend primarily on the jet size as well as on the

polymer content in the jet. During the travelling of a solution jet from the syringe to the metal collector, the primary jet may or may not split into multiple jets, resulting in different fibres diameters. As long as no splitting is involved, one of the most significant parameters influencing the fibres diameter is the solution viscosity. A higher viscosity results in a larger fibre diameter. When a solid polymer is dissolved in a solvent, the solution viscosity is directly proportional to its concentration. According to this, the higher the polymer concentration, the larger the resulting nanofibres diameters will be.

Attending to the solvent ratio, the fibre diameter increases when the content of non-polar solvent (be it chloroform or DCM) increases in the solvent mixture. The effect of the solvent ratio on the diameter can be explained in terms of their dielectric constants [38]. Those of chloroform and DCM are 4.8 and 9.1, respectively, whereas those of methanol and DMF are 32.6 and 36.7, respectively, [39] and the thicker fibres appear when the solvent binary mixture is rich in a solvent with low dielectric constant. Indeed, solutions richer in solvents with low dielectric constant are expected to have lower conductivity, resulting in a lesser stretching of the jet. Additionally, the enrichment of the mixture in a non-polar solvent implies an increment of viscosity due to the lower solubility of the polymer.

The effect of these electrospinning parameters on the fibres diameter is clearly shown in Figure 4. For PCL, using chloroform-methanol as solvents, it is possible to obtain fibres with under-micron diameter until 15% wt/v of polymer concentration with a low content in chloroform (66:33 %v/v). However, to obtain fibres with above-micron diameter with 15% wt/v of PCL the content of chloroform should be increased, indeed the 75:25 %v/v ratio results in fibres diameters above two microns. That is, these parameters have to be changed in order to tailor the solution to the required fibres

diameter. Figure 4 also shows the influence of the main electrospinning process parameters (flow rate, voltage and distance to collector) on fibres diameter. Only increasing the flow rate, the diameter increases, although with a weak effect. For this reason, the modification of this parameter is the final step to adjust the fibre diameter to the targeted specifications. Flow rates of 2 – 3 ml/h yield above-micron diameters, so to reduce the diameter below the micron other parameters have rather to be modified. A low flow rate is in general more recommended as the polymer solution gets enough time for polarization. [40] Conversely, if the flow rate is too high, beads and thicker fibres form owing to the short drying time before reaching the collector and subsequent low stretching forces.

Another key parameter is voltage, which allows reducing significantly the fibres diameter by increasing it. The formation of smaller-diameter nanofibres in response to an increase in the applied voltage is attributed to the stretching of the polymer solution in correlation with the charge repulsion within the polymer jet. [41] For 15%wt/v PLA (in 66:33 %v/v chloroform-methanol) electrospun membranes the lowest diameter obtained is 1.3 µm for 25 kV, growing up to 1.8 µm for 20 kV, so electrospun membranes with under-micron fibres can be rather achieved by varying other parameters.

The distance to collector is indirectly correlated with the fibres diameter, since it influences both the shape and intensity of the electric field and the total flight time available to the electrospinning jet. A reduction of the electrode distance can result in the suppression of the later stages of fibre elongation and solvent evaporation. Generally this leads to increased fibre diameter and adhesion both to other fibres and the collector, due to incomplete solvent evaporation. [42] The influence of this parameter is almost negligible herein: increasing 7 cm de distance to the collector the diameter is reduced only about 0.1 µm. For this reason, it is possible to work in a range of 13 to 20 cm to

collector obtaining electrospun membranes with above-micron diameters in all cases. It would be necessary to change other parameters to fabricate membranes with under-micron diameters.

Due to the fact that the solvent ratio and voltage do significantly modify the diameters, they were varied in a first approach. When the diameter of electrospun membranes were near to the established fibre diameter, the polymer concentration, flow rate and distance to the collector were finely tailored. The selected parameters of electrospinning to get above- and under-micron fibres without defects are included in Table 1.

Table 1. Optimal electrospinning parameters (polymer concentration (%wt/v), solvents and their ratio (%v), flow rate, distance to collector and voltage) to obtain membranes having 0.8 and 1.8 µm fibres diameters.

Membranes U (ϕ = 0.8 µm)	**Membranes A (ϕ = 1.8 µm)**
PLA 8% chloroform-methanol (66:33)	PLA 15% chloroform-methanol (66:33)
2 ml/h	2 ml/h
13 cm	13 cm
25 kV	20 kV
PLAPCL 12% DCM-DMF (75:25)	PLAPCL 20% DCM-DMF (75:25)
2 ml/h	2 ml/h
15 cm	15 cm
25 kV	20 kV
PCL 10% chloroform-methanol (70:30)	PCL 15% chloroform-methanol (66:33)
2 ml/h	2 ml/h
13 cm	13 cm
25 kV	25 kV

Figure 5 shows SEM images of these electrospun membranes and the histograms of fibres diameters after their analyses using the ImageJ software. Membranes having two different fibre diameters (0.8 and 1.8 µm) were successfully fabricated by modifying the main electrospinning parameters. Moreover, no defects in membranes, such as drops, are observed.

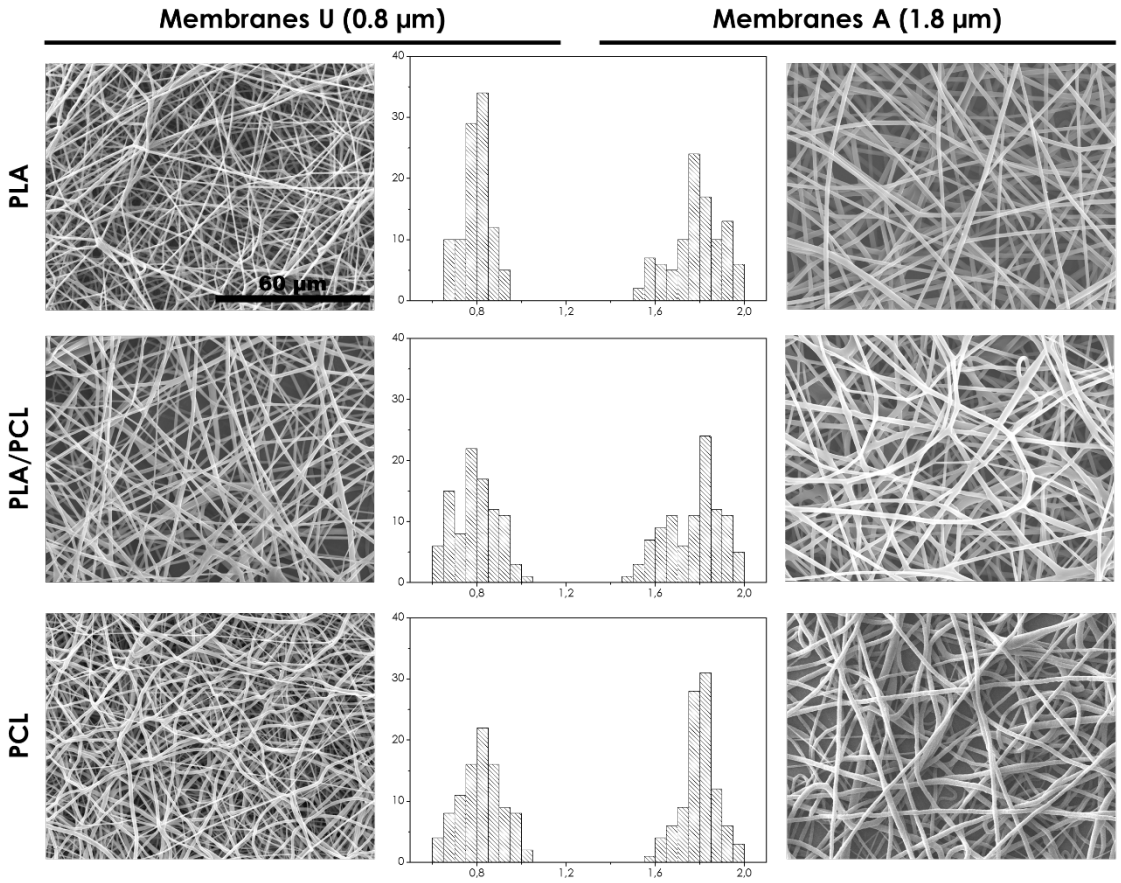

Figure 5. Histograms of fibres diameters (number of fibres vs. fibre diameter in µm) and SEM images of the non-loaded electrospun membranes U (under-micron fibres), on the left, and A (above-micron), on the right. Scale bar: 60 µm in all images.

3.2. Characterisation of the polymer solutions

The rheograms of the polymer solutions leading to membranes with 0.8 µm and 1.8 µm in diameter (those of Table 1) were obtained (curves not shown). They showed that polymer solutions are no-newtonian fluids because the viscosity decreases with the shear rate. [43] From these data, the viscosity of each mixture was determined at a shear rate of 710 s^{-1}, and the results are shown in Table 2.

European Polymer Journal 99 (2018) 445–455
https://doi.org/10.1016/j.eurpolymj.2017.12.045

Table 2. Viscosity (Pa·s) of the polymer solutions in Table 1 at a shear rate of 710 s^{-1}.

	U membranes	A membranes
PLA	0.373 ± 0.012	1.175 ± 0.024
PLA/PCL	0.227 ± 0.034	1.037 ± 0.069
PCL	0.410 ± 0.013	1.045 ± 0.025

A high viscosity (around 1 Pa·s) of the polymer solutions implies thicker diameters (1.8 μm) of the fibres in their electrospun membranes. The increased viscosity of the more concentrated solutions creates higher viscoelastic forces that resist the axial stretching during whipping, resulting in larger fibre diameters, as described in. [44]

To assess the influence of the chemical nature of the polymer, solutions of PLA and PCL leading to membranes A were considered, since the polymer concentration, the solvents and the ratio between solvents are the same in both. In this way, we can say that PLA increases slightly the viscosity of the mixture with respect to PCL. This can be attributed to the fact that PLA, having a lower CHx/COOH ratio than PCL, has a worse affinity for a solvents mixture concentrated in an apolar solvent (chloroform) with a polar one (methanol). Besides, the polymer concentration plays a main role in the viscosity of the polymeric solution, as expected. In fact, an increment of PLA concentration in 87.5% entailed an increment of 215% in the viscosity of its solution.

Finally, the use of DCM-DMF as solvents allows increasing the polymer concentration without any influence in the viscosity of polymeric solution, probably for the polar but aprotic nature of DMF.

Figure 6 displays the surface tension of the polymer solutions chosen to get the U and A membranes, previously listed in Table 1. As expected, a higher surface tension of polymer solutions yields membranes with greater fibres diameters. This is caused by the

difficulty to eject the polymeric solution since the applied voltage must exceed the surface tension. [45]

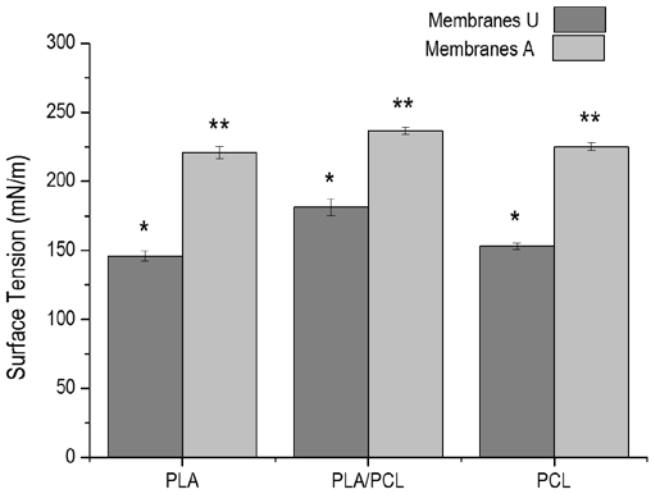

Figure 6. Surface tension (mN/m) obtained by applying Tate's Law, of polymer solutions prepared to electrospin U and A membranes.

The polymer concentration is decisive in the value of the surface tension, so that to obtain membranes with high fibre diameters (high surface tension), the polymer concentration must be increased. However, the significance of the polymer concentration on the surface tension of the solution depends on the polymer used. As an example, an increment of 87.5% in PLA concentration involves an increment of 51.3% on the surface tension, whereas when modifying the solvent ratio, an increment of 47% on the surface tension was achieved by increasing by 50% the polymer concentration (in case of PCL). Hence, varying the solvent ratio it is possible to reduce the polymer concentration required to obtain certain fibre diameters.

Finally, when DCM-DMF are used as solvents, solutions with higher surface tension are needed to get fibres with the same diameter.

3.3. BSA release from membranes with tailored fibres diameter

To explore whether differences in fibres diameter around one micron could raise different strategies in terms of drug release, firstly the chosen electrospinning parameters were redefined in order to allow the incorporation of BSA whilst keeping the mean fibres diameter. However, the loading of BSA was not a trivial matter, since it is not soluble in the organic solvents used to dissolve the polymers. Thus, a surfactant was required and its concentration, as well as the procedure to obtain the solution, had to be set. It was found that *i)* Span80 worked well as surfactant in these mixtures whereas Tween80 did not, *ii)* a minimum concentration of 40% wt with respect to BSA was required, and *iii)* it had to be incorporated to the polymer solution before adding the BSA aqueous solution and not afterwards. Indeed, compared to Tween80, Span80 has a more lipophilic character: according to [46], the hydrophile-lipophile balance (HLB number) of Span80 is 4.3, whereas that of Tween80 is 15 and thus does not emulsify these mixtures. In [47], the authors investigated the release behavior of BSA encapsulated in emulsion electrospun poly(L-lactide-co-caprolactone) fibers, using chloroform, and did successfully use Span80 as well.

The membranes loaded with BSA (Figure 7) show and identical appearance to those of non-loaded membranes. However, it was necessary to modify the flow rate of the BSA-loaded PCL solution to obtain its U membranes, from 2 to 4 ml/h; otherwise the fibre diameter dropped to 0.42±0.08 μm.

European Polymer Journal 99 (2018) 445–455
https://doi.org/10.1016/j.eurpolymj.2017.12.045

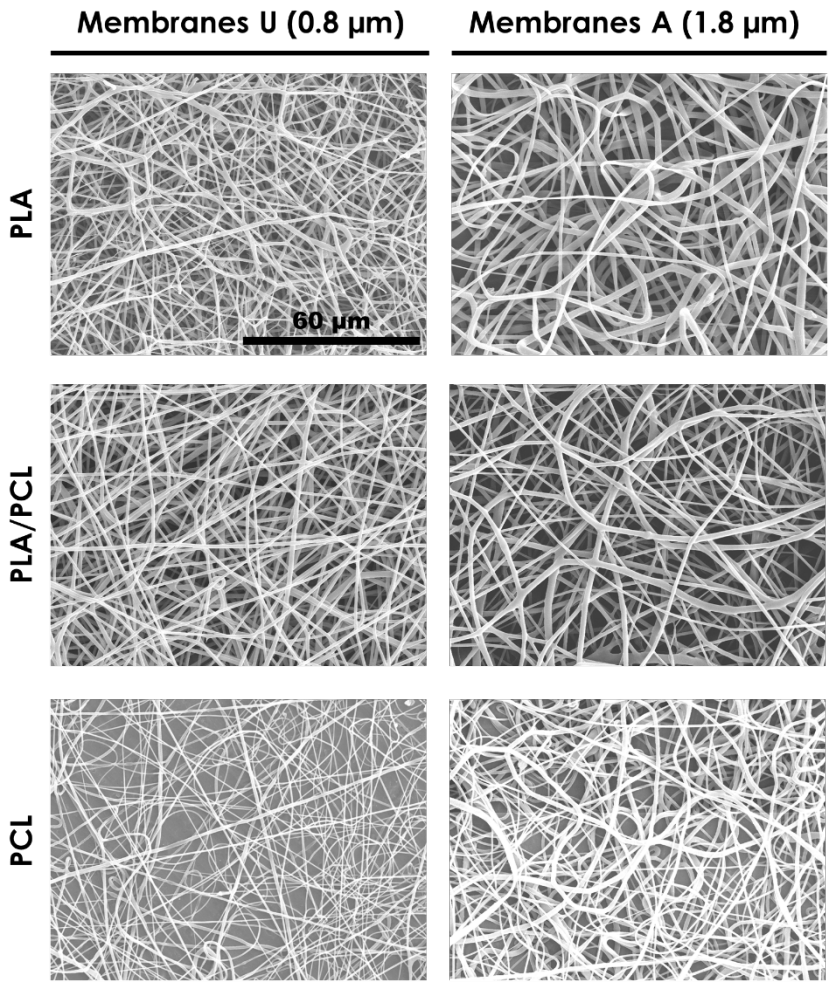

Figure 7. SEM images showing the morphology of BSA-loaded U and A electrospun membranes. Scale bar: 60 µm.

Once the electrospinning parameters had been redefined to obtain the specific fibre diameters, the membranes were immersed in PBS to follow the release of BSA. The release of BSA was in parallel followed from films of the polymers. Figure 8 shows the mass fraction of BSA released at different time points throughout the experiment.

European Polymer Journal 99 (2018) 445–455
https://doi.org/10.1016/j.eurpolymj.2017.12.045

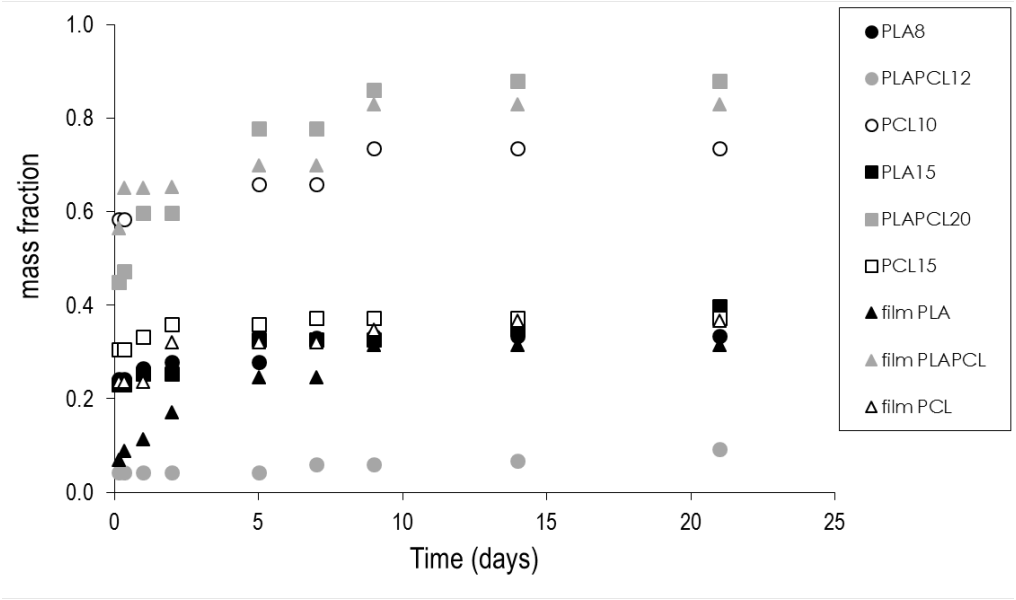

Figure 8. Evolution of the release of BSA with time, expressed in terms of mass fraction with respect to the mass initially incorporated, through loaded membranes and films.

On the one hand, the release of BSA occurs at a greater extent at short times, below 5 days. On the other hand, in electrospun PLA the diameter of fibres affects the release only at short times, from PCL the highest release of BSA occurs from smaller fibre diameters, but PLA/PCL shows the opposite behaviour: the lowest release of BSA occurs from smaller fibre diameters.

The percentage of cumulative BSA released after 21 days is gathered in Table 3.

Table 3. Cumulative BSA released (% on the basis of the loaded BSA) from membranes after 21 days.

	Membranes U	**Membranes A**	**Films**
PLA	33.5%	39.7%	31.5%
PLA/PCL	9.3%	87.9%	83.1%
PCL	73.5%	37.2%	36.7%

The greatest release was obtained from electrospun A PLA/PCL membranes and films. The deviation of U membranes with respect to this behaviour can be attributed to the difficulty to maintain the stability of the latter emulsion. The different release behaviour

of pure polymers can be explained in terms of the solvents used. DCM-DMF have distant boiling points, 40 and 153ºC, respectively, [39] leading to phase separation and resulting in the fabrication of highly porous electrospun nanofibres, [41] which facilitate the release of BSA.

Only from PCL membranes a higher release rate was observed from smaller-sized fibres, as expected given its higher surface/volume ratio, which facilitated the release of BSA as PCL is surface hydrolysed.

Figure 9 shows the calorimetric curves for PCL, PLA and the PLA/PCL mixture, the last showing the two melting peaks at approximately 60ºC and 150ºC, corresponding to PCL and PLA, respectively. Those of PLA membranes show a crystallization peak at 90-100ºC (framed area) probably due to chain orientations. [48]

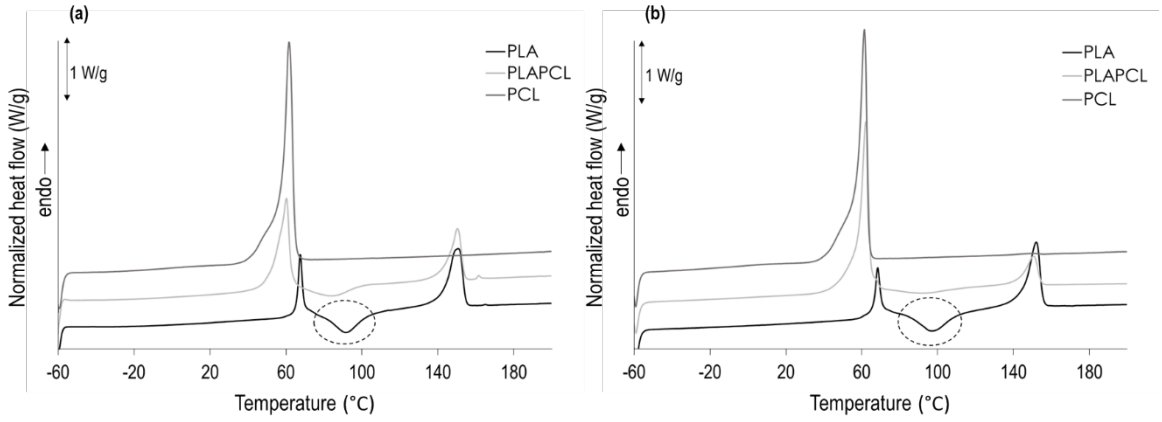

Figure 9. Calorimetric curves for (a) U- and (b) A-membranes.

In terms of crystallinity, PCL membranes have higher crystallinity (54.6% for U-membranes and 53.0% for A- ones) than PLA (17.8% for U-membranes and 14.2% for A- ones). A small increment in the fibre diameter seems to deliver slightly less crystalline membranes. In the PLA/PCL blend, the crystallinity becomes 28.3% for its PLA chains and 46.8% for PCL ones, averaged 37.6% in case of U-membranes, and

20.5% for PLA and 73.2% for PCL in A-membranes, averaged 46.9%. These values are between those obtained for PCL and PLA. The crystallinity of the blends does not seem to explain the behaviour observed in terms of BSA release, which, as stated before, rather responds to the variable porosity of their membranes.

4. CONCLUSIONS

PLA, PCL and PLA/PCL electrospun membranes were successfully obtained, with sub- and above- micron diameters, varying the main electrospinning parameters. After analysing these variables it can be stated that the solvent ratio (chloroform:methanol or DCM:DMF) and voltage have both a great influence on the fibres diameters, so to tailor membranes with specific diameters they should be the foremost to scan.

Increasing the polymers concentration in a chloroform/methanol binary mixture allows increasing the viscosity and surface tension of the mixture and thus the diameter of its electrospun fibres. Swapping to DCM/DMF enables to concentrate the solution more without significantly changing its viscosity.

With regard to the application of these membranes to release a molecule of interest, the stability of the emulsion to electrospin is the main aspect to consider. In particular, PLA/PCL membranes with above-micron fibres were found to be the most effective configuration to release BSA.

ACKNOWLEDGMENTS

The authors acknowledge Spanish Ministerio de Economía y Competitividad through DPI2015-65401-C3-2-R project, and the assistance and advice of the Electron Microscopy Service of the Universitat Politècnica de València (Spain).

REFERENCES

1. Drumright, R. E., Gruber, P. R. & Henton, D. E. Polylactic acid technology. *Adv. Mater.* **12,** 1841–1846 (2000).
2. Bawa, K. K. & Oh, J. K. Stimulus-Responsive Degradable Polylactide-Based Block Copolymer Nanoassemblies for Controlled / Enhanced Drug Delivery. *Mol. Pharm.* (2017). doi:10.1021/acs.molpharmaceut.7b00284
3. Uhrich, K. E., Cannizzaro, S. M., Langer, R. S. & Shakesheff, K. M. Polymeric Systems for Controlled Drug Release. *Chem. Rev.* **99,** 3181–3198 (1999).
4. Jacobson, G. B., Shinde, R., Contag, C. H. & Zare, R. N. Sustained release of drugs dispersed in polymer nanoparticles. *Angew. Chemie - Int. Ed.* **47,** 7880–7882 (2008).
5. Odile Dechy-Cabaret , Blanca Martin-Vaca, and D. B. Controlled Ring-Opening Polymerization of Lactide and Glycolide. *Am. Chem. Soc.* **104,** 6147–6176 (2004).
6. Gunatillake, P. A., Adhikari, R. & Gadegaard, N. Biodegradable synthetic polymers for tissue engineering. *Eur. Cells Mater.* **5,** 1–16 (2003).
7. Hutmacher DW Schantz T, Z. I. N. K. W. T. S. H. T. K. C. Mechanical properties and cell cultural response of polycalrolactone scaffolds designed and fabricated via fused deposition modelling. *J. Biomedial Mater. Res.* **55,** 203–216 (2001).
8. Mohamed, R. M. & Yusoh, K. A Review on the Recent Research of Polycaprolactone (PCL). *Adv. Mater. Res.* **1134,** 249–255 (2015).
9. Ren, K., Wang, Y., Sun, T., Yue, W. & Zhang, H. Electrospun PCL/gelatin composite nanofiber structures for effective guided bone regeneration membranes. *Mater. Sci. Eng. C* **78,** 324–332 (2017).
10. Fereshteh, Z., Fathi, M., Bagri, A. & Boccaccini, A. R. Preparation and

characterization of aligned porous PCL/zein scaffolds as drug delivery systems via improved unidirectional freeze-drying method. *Mater. Sci. Eng. C* **68,** 613–622 (2016).

11. Salerno, A., Domingo, C. & Saurina, J. PCL foamed scaffolds loaded with 5-fluorouracil anti-cancer drug prepared by an eco-friendly route. *Mater. Sci. Eng. C* **75,** 1191–1197 (2017).
12. Stafiej, P. *et al.* Adhesion and metabolic activity of human corneal cells on PCL based nanofiber matrices. *Mater. Sci. Eng. C* **71,** 764–770 (2017).
13. Morelli, S., Salerno, S., Holopainen, J., Ritala, M. & De Bartolo, L. Osteogenic and osteoclastogenic differentiation of co-cultured cells in polylactic acid-nanohydroxyapatite fiber scaffolds. *J. Biotechnol.* **204,** 53–62 (2015).
14. Tyler, B., Gullotti, D., Mangraviti, A., Utsuki, T. & Brem, H. Polylactic acid (PLA) controlled delivery carriers for biomedical applications. *Adv. Drug Deliv. Rev.* **107,** 163–175 (2016).
15. Woodruff, M. A. & Hutmacher, D. W. The return of a forgotten polymer - Polycaprolactone in the 21st century. *Prog. Polym. Sci.* **35,** 1217–1256 (2010).
16. Li, W. J., Laurencin, C. T., Caterson, E. J., Tuan, R. S. & Ko, F. K. Electrospun nanofibrous structure: A novel scaffold for tissue engineering. *J. Biomed. Mater. Res.* **60,** 613–621 (2002).
17. He, W., Horn, S. W. & Hussain, M. D. Improved bioavailability of orally administered mifepristone from PLGA nanoparticles. *Int. J. Pharm.* **334,** 173–178 (2007).
18. Shakhssalim, N. *et al.* Bladder smooth muscle cells on electrospun poly(ε-caprolactone)/poly(l-lactic acid) scaffold promote bladder regeneration in a canine model. *Mater. Sci. Eng. C. Mater. Biol. Appl.* **75,** 877–884 (2017).

19. Bhardwaj, N. & Kundu, S. C. Electrospinning: A fascinating fiber fabrication technique. *Biotechnol. Adv.* **28,** 325–347 (2010).

20. Liang, D., Hsiao, B. S. & Chu, B. Functional electrospun nanofibrous scaffolds for biomedical applications. *Adv. Drug Deliv. Rev.* **59,** 1392–1412 (2007).

21. Subbiah, T., Bhat, G. S., Tock, R. W., Parameswaran, S. & Ramkumar, S. S. Electrospinning of nanofibers. *J. Appl. Polym. Sci.* **96,** 557–569 (2005).

22. Chong, E. J. *et al.* Evaluation of electrospun PCL/gelatin nanofibrous scaffold for wound healing and layered dermal reconstitution. *Acta Biomater.* **3,** 321–330 (2007).

23. Sankaran, K. K., Krishnan, U. M. & Sethuraman, S. Axially aligned 3D nanofibrous grafts of PLA-PCL for small diameter cardiovascular applications. *J. Biomater. Sci. Polym. Ed.* **25,** 1791–1812 (2014).

24. Guo, C., Zhou, L. & Lv, J. Effects of expandable graphite and modified ammonium polyphosphate on the flame-retardant and mechanical properties of wood flour-polypropylene composites. *Polym. Polym. Compos.* **21,** 449–456 (2013).

25. Zhu, R. T. *et al.* Morphological Structure and Thermal Property of PLA/PCL Nanofiber by Electrospinning. *Adv. Mater. Res.* **1048,** 418–422 (2014).

26. Hadjizadeh, A. & Doillon, C. J. Directional migration of endothelial cells towards angiogenesis using polymer fibres in a 3D co-culture system. *J. Tissue Eng. Regen. Med.* **4,** 524–531 (2010).

27. Gómez-Tejedor, J. A., Overberghe, N. Van, Rico, P. & Ribelles, J. L. G. Assessment of the parameters influencing the fiber characteristics of electrospun poly(ethyl methacrylate) membranes. *Eur. Polym. J.* **47,** 119–129 (2011).

28. Areias, A. C. *et al.* Assessment of parameters influencing fiber characteristics of

chitosan nanofiber membrane to optimize fiber mat production. *Polym. Eng. Sci.* (2012). doi:10.1002/pen

29. Silva, C. S. R. *et al.* Poly(ε-caprolactone) electrospun scaffolds filled with nanoparticles. Production and optimization according to Taguchi's methodology. *J. Macromol. Sci. Part B* **53,** 781–799 (2014).

30. Ramakrishna, S., Fujihara, K., Teo, W. E., Lim, T. C. & Ma, Z. An introduction to electrospinning and nanofibers. *World Sci. Singapore* (2005).

31. Riba, J.-R. & Esteban, B. A simple laboratory experiment to measure the surface tension of a liquid in contact with air. *Eur. J. Phys.* **35,** 55003 (2014).

32. Earnshaw, J. C., Johnson, E. G., Carroll, B. J. & Doyle, P. J. The drop volume method for interfacial tension determination: an error analysis. *J. Colloid Interface Sci.* **177,** 150–155 (1996).

33. Lee, B. B., Ravindra, P. & Chan, E. S. New drop weight analysis for surface tension determination of liquids. *Colloids Surfaces A Physicochem. Eng. Asp.* **332,** 112–120 (2009).

34. Simoes, C.L., Viana, J.C. & Cunha, A.M. Mechanical properties of poly (e-caprolactone) and poly(lactic acid) blends. *J. Appl. Polym. Sci.* **112**, 345-352 (2009).

35. Zhai, W., Ko, Y., Zhu, W., Wong, A. & Park, C. B. A study of the crystallization, melting, and foaming behaviors of polylactic acid in compressed CO2. *Int. J. Mol. Sci.* **10,** 5381–5397 (2009).

36. Gupta, B., Geeta & Ray, A. R. Preparation of Poly(e-caprolactone)/Poly(e-caprolactone-co-lactide) (PCL/PLCL) blend filament by melt spinning. *Appl. Polym. Sci.* **123,** 1944–1950 (2012).

37. Huang, Z. M., Zhang, Y. Z., Kotaki, M. & Ramakrishna, S. A review on polymer

nanofibers by electrospinning and their applications in nanocomposites. *Compos. Sci. Technol.* **63,** 2223–2253 (2003).

38. Veleirinho, B., Rei, M. F. & Lopes-da-Silva, J. A. Solvent and concentration effects on the properties of electrospun poly(ethylene terephthalate) nanofiber mats. *J. Polym. Sci. Part B Polym. Phys.* **46,** 460–471 (2008).

39. Comyn, J. Handbook of organic solvent properties. *Int. J. Adhes. Adhes.* **17,** 177 (1997).

40. Li, Z. & Wang, C. Effects of working parameters on electrospinning. in *One-Dimensional nanostructures* (Springer, 2013).

41. Haider, A., Haider, S. & Kang, I. K. A comprehensive review summarizing the effect of electrospinning parameters and potential applications of nanofibers in biomedical and biotechnology. *Arab. J. Chem.* (2015). doi:10.1016/j.arabjc.2015.11.015

42. Burke, L., Keshvari, A., Hilal, N. & Wright, C. J. Electrospinning: A practical approach for membrane fabrication. in *Membrane Fabrication* (eds. Hilal, N., Ismal, A. F. & Wright, C.) 45–74 (RC Press, 2015).

43. Rojas, O. *Introducción a la reología*. (Laboratorio FIRP, Universidad de los Andes, 1999).

44. Nezarati, R. M., Eifert, M. B. & Cosgriff-Hernandez, E. Effects of Humidity and Solution Viscosity on Electrospun Fiber Morphology. *Tissue Eng. Part C Methods* **19,** 810–819 (2013).

45. Fong, H., Chun, I. & Reneker, D. H. Beaded nanofibers formed during electrospinning. *Polymer*. **40,** 4585–4592 (1999).

46. *The HLB system: a time-saving guide to emulsifier selection*. (ICI Americas Inc., 1976). Chapter 1.

47. Xiaoqianga, L., Yan, S., Shuiping, L., Lianjiang, T., Xiumei, M. & Ramakrishna, S. Encapsulation of proteins in poly(l-lactide-co-caprolactone) fibers by emulsion electrospinning. *Colloids Surf. B Biointerfaces*. **75**, 418–424 (2010).

48. Zong, X., Kim, K., Fang, D., Ran, S., Hsiao, B. S. & Chu, B. Structure and process relationship of electrospun bioabsorbable nanofiber membranes. *Polymer*. **43,** 4403–4412 (2002).